



An alternative approach to modeling radiation from baffled circular pistons (L)

Chirag A. Gokani,^{1,2,a)} Randall P. Williams,^{1,2} Michael R. Haberman,^{1,2}  and Mark F. Hamilton^{1,2} 

¹Applied Research Laboratories, The University of Texas at Austin, Austin, Texas 78766-9767, USA

²Walker Department of Mechanical Engineering, The University of Texas at Austin, Austin, Texas 78712-1063, USA

ABSTRACT:

The study of radiation from baffled circular pistons often begins with the Rayleigh integral. The present letter offers an alternative derivation of the Rayleigh integral by solving the Helmholtz equation for a baffled circular piston in an infinitely large cylindrical waveguide. While the Rayleigh integral is typically interpreted as a sum of simple sources, the present derivation shows that the Rayleigh integral can also be cast as a sum of Bessel beams. The alternative formulation is used to recover the axial pressure radiated by a baffled circular piston and solve the Helmholtz equation numerically for a vortex beam. © 2025 Acoustical Society of America.

<https://doi.org/10.1121/10.0039425>

(Received 21 July 2025; revised 5 September 2025; accepted 5 September 2025; published online 30 September 2025)

[Editor: Philip L. Marston]

Pages: 2642–2646

I. INTRODUCTION

Radiation of sound from a baffled circular piston is a canonical problem in acoustics.¹ Fields radiated by circular pistons continue to be studied² and widely applied.^{3,4} Analytical solutions were derived recently in the far field based on the paraxial approximation for radiation from time-harmonic sources whose velocity in the z direction is described in cylindrical coordinates (r, θ, z) by⁵

$$u_z(r, \theta, 0) = u_0 \text{circ}(r/a) e^{i\ell\theta}, \quad (1)$$

where $\text{circ}(r/a) = 1$ for $0 < r/a \leq 1$ and 0 elsewhere, a is the radius of the piston, and ℓ is the orbital number, which is nonzero for vortex beams.^{6,7} With zero amplitude assigned at $r = 0$, the ambiguity in phase at $r = 0$ for $\ell \neq 0$ is avoided without affecting the integrations in the following analysis.

The Rayleigh integral⁸

$$p(\mathbf{r}) = -\frac{ik\rho_0 c_0}{2\pi} \int_{S_0} u_z(\mathbf{r}_0) \frac{e^{ik|\mathbf{r}-\mathbf{r}_0|}}{|\mathbf{r}-\mathbf{r}_0|} dS_0 \quad (2)$$

is an exact solution of the Helmholtz equation and is often the starting point for obtaining the time-harmonic pressure p radiated in an infinite half-space, where k is the wavenumber, ρ_0 is the ambient density of the fluid, c_0 is the sound speed, and S_0 is the radiating surface in the source plane $z = 0$. Equation (2) is traditionally derived from the Helmholtz–Kirchhoff integral.⁸ In the present letter, Eq. (2) is obtained for the case of a circular piston by considering a different problem, a piston described by Eq. (1) placed concentrically within a pressure-release waveguide of radius b

as shown in Fig. 1. A piston in an infinite baffle is obtained in the limit as $b \rightarrow \infty$, whereupon the sum of modes in the waveguide becomes an integral in free space over the cylindrical eigenfunctions of the Helmholtz equation.

The recovery of Eq. (2) from the modal solution demonstrates that diffraction theory can be viewed as a limiting case of modal analysis. Starting with the modal solution draws a parallel with the solution of the paraxial equation in terms of Laguerre–Gaussian modes^{6,9} and provides a natural way of describing diffraction in cylindrical coordinates. The representation of Eq. (2) in terms of the cylindrical eigenfunctions of the Helmholtz equation is amenable to problems with cylindrical features and rotational symmetry, including scattering.^{10,11} The present work also simplifies the numerical evaluation of Eq. (2) for sources described by Eq. (1) by reducing the surface integral to an integral over a single variable.

The modal solution of the Helmholtz equation for the piston in the waveguide of finite radius b is obtained in Sec. II. The limit $b \rightarrow \infty$ is taken in Sec. III, and Eq. (2) is recovered in Sec. IV. Two examples that demonstrate the utility of the present formulation follow in Sec. V.

II. MODAL SOLUTION IN WAVEGUIDE

The general solution of the Helmholtz equation for the geometry depicted in Fig. 1 is¹²

$$p(r, \theta, z) = \sum_{q=-\infty}^{\infty} \sum_{m=1}^{\infty} A_{qm} J_q(\alpha_{qm} r/b) e^{i(q\theta + \beta_{qm} z)}, \quad (3)$$

where α_{qm} is the m th root of the Bessel function of order q , and where $\beta_{qm} = \sqrt{k^2 - (\alpha_{qm}/b)^2}$ is the z component of the wave vector. For Eq. (3) to equal Eq. (1) in the source plane, set $q = \ell$ and $u_z = (ik\rho_0 c_0)^{-1} \partial p / \partial z|_{z=0}$:

^{a)}Email: chiragokani@utexas.edu

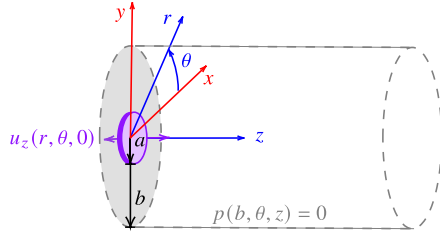


FIG. 1. Baffled circular piston of radius a in the plane $z = 0$ with normal velocity amplitude u_0 . The piston is concentric within a pressure-release cylindrical waveguide of radius b .

$$\sum_{m=1}^{\infty} A_{\ell m} \beta_{\ell m} J_{\ell}(\alpha_{\ell m} r/b) = k \rho_0 c_0 u_0 \text{circ}(r/a). \quad (4)$$

Multiplication of Eq. (4) by $r J_{\ell}(\alpha_{\ell n} r/b)$, integration over r from 0 to b , and use of the orthogonality relation¹³ $\int_0^b J_{\ell}(\alpha_{\ell m} r/b) J_{\ell}(\alpha_{\ell n} r/b) r dr = (b^2/2) \delta_{mn} J_{\ell+1}^2(\alpha_{\ell n})$, yields

$$A_{\ell n} \beta_{\ell n} J_{\ell+1}^2(\alpha_{\ell n}) = 2k \rho_0 c_0 u_0 \alpha_{\ell n}^{-2} F_{\ell}(\alpha_{\ell n} a/b) \quad (5)$$

for $\ell > -2$, where δ_{mn} is the Kronecker delta, and where $F_{\ell}(\zeta) = \int_0^{\zeta} J_{\ell}(t) t dt$ is given by Eqs. (7) and (8) of Ref. 5. Solving Eq. (5) for $A_{\ell n}$ yields the solution of the Helmholtz equation for the geometry shown in Fig. 1:

$$p(r, \theta, z) = \sum_{n=1}^{\infty} A_{\ell n} J_{\ell}(\alpha_{\ell n} r/b) e^{i(\ell\theta + \beta_{\ell n} z)}, \quad (6)$$

$$A_{\ell n} = 2\rho_0 c_0 u_0 \frac{k}{\alpha_{\ell n}^2 \beta_{\ell n}} \frac{F_{\ell}(\alpha_{\ell n} a/b)}{J_{\ell+1}^2(\alpha_{\ell n})}, \quad (7)$$

$$\beta_{\ell n} = \sqrt{k^2 - (\alpha_{\ell n}/b)^2}. \quad (8)$$

III. LIMIT OF INFINITE WAVEGUIDE RADIUS

The limit $b \rightarrow \infty$ of Eq. (6) corresponds to the field radiated into an infinite half-space and is obtained by noting that the ratio $\alpha_{\ell n}/b$ appearing in Eqs. (6)–(8) is vanishingly small, except for large n , for which¹³

$$\alpha_{\ell n} \simeq \pi(n - 1/4 + \ell/2), \quad n \gg 1. \quad (9)$$

Introducing the dimensionless parameter

$$\zeta = \frac{a}{b} \pi(n - 1/4 + \ell/2) \quad (10)$$

permits Eqs. (7) and (8) to be written for large n as

$$A_{\ell n} \simeq \rho_0 c_0 u_0 \frac{\Delta \zeta}{\zeta} \frac{F_{\ell}(\zeta)}{\sqrt{1 - (\zeta/ka)^2}}, \quad (11)$$

$$\beta_{\ell n} \simeq k \sqrt{1 - (\zeta/ka)^2}, \quad n \gg 1, \quad (12)$$

respectively, where $\Delta \zeta = \pi a/b$, and where the relation¹⁴

$$J_{\nu}(x) \simeq \sqrt{\frac{2}{\pi x}} \cos(x - \nu\pi/2 - \pi/4), \quad x \gg 1 \quad (13)$$

has been used to obtain the asymptotic form of $J_{\ell+1}(\alpha_{\ell n})$ appearing in Eq. (7):

$$\frac{1}{J_{\ell+1}^2(\alpha_{\ell n})} \simeq \frac{\pi^2}{2} (n - 1/4 + \ell/2), \quad n \gg 1. \quad (14)$$

Inserting Eqs. (10)–(12) into Eq. (6) yields

$$p = \rho_0 c_0 u_0 e^{i\ell\theta} \sum_{n=1}^{\infty} \frac{\Delta \zeta}{\zeta} \frac{F_{\ell}(\zeta) J_{\ell}(\zeta r/a)}{\sqrt{1 - (\zeta/ka)^2}} e^{ikz \sqrt{1 - (\zeta/ka)^2}}. \quad (15)$$

In the limit $b \rightarrow \infty$, $\Delta \zeta$ becomes $d\zeta$, and the summation becomes an integral:

$$p = \rho_0 c_0 u_0 e^{i\ell\theta} \int_0^{\infty} \frac{F_{\ell}(\zeta) J_{\ell}(\zeta r/a)}{\zeta \sqrt{1 - (\zeta/ka)^2}} e^{ikz \sqrt{1 - (\zeta/ka)^2}} d\zeta. \quad (16)$$

Noting from Eqs. (8), (10), and (12) that $\zeta = k_r a$ and $\sqrt{1 - (\zeta/ka)^2} = k_z/k$, where k_r and k_z are the r and z components of the wave vector, respectively, allows Eq. (16) to be expressed as

$$p = \rho_0 c_0 u_0 e^{i\ell\theta} k \int_0^{\infty} F_{\ell}(k_r a) J_{\ell}(k_r r) \frac{e^{ik_z z}}{k_z k_r} dk_r. \quad (17)$$

Equation (17) is equivalent to the Rayleigh integral, as shown in Sec. IV. While the Rayleigh integral is traditionally interpreted as the “sum of the radiations from...individual simple sources,”¹² Equation (17) shows that the Rayleigh integral can also be viewed as a sum of the eigenfunctions $J_{\ell}(k_r r) e^{i(\ell\theta + k_z z)}$ of the Helmholtz equation. The eigenfunctions are also known as Bessel beams,¹⁰ which are convenient for analysis because they do not diffract.¹⁵ Equation (17) can then be interpreted as the Bessel-beam decomposition of the field radiated by a source described by Eq. (1). Studies involving individual Bessel beams may be generalized using Eq. (17) to fields radiated by circular pistons, although the superposition principle underlying such a decomposition requires that the wave phenomenon of interest be linear.¹⁶

The Bessel-beam decomposition of radiation from a circular pressure source for $\ell = 0$ was previously derived by King,¹⁷ Junger and Feit,¹⁸ and Daniel *et al.*¹¹ Setting $\ell = 0$ in Eq. (17) and identifying $k_r = \lambda$, $ik_z = \mu$, $u_z = -(\partial\phi/\partial z)|_{z=0}$, $p = ik\rho_0 c_0 \phi$, and $u_0 = \dot{x}$ recovers Eq. (5) of Ref. 17, where the convention $i(\omega t - kz)$ used in Ref. 17 explains the minus sign in the exponential of Eq. (5). Similarly, identifying $k_r = \gamma$ and $-ikc_0 u_0 = \dot{W}$ recovers Eq. (5.16) in combination with Eq. (5.4) of Ref. 18. Meanwhile, denoting $k_r = k \sin \beta$ and $k_z = k \cos \beta$ recovers Eq. (3) in combination with Eq. (B-5) of Ref. 11, where the additional factor of $\cos \beta$ in Eq. (B-5)

appears because a pressure source is considered in Ref. 11, whereas a velocity source is considered in Refs. 17 and 18 and the present work.

Equation (17) is also obtained if the boundary at $r = b$ is rigid ($\partial p / \partial r|_{r=b} = 0$), in which case the modal solution of the Helmholtz equation is

$$p(r, \theta, z) = \sum_{n=1}^{\infty} A'_{\ell n} J_{\ell}(\alpha'_{\ell n} r / b) e^{i(\ell\theta + \beta'_{\ell n} z)}, \quad (18)$$

$$A'_{\ell n} = \frac{2\rho_0 c_0 u_0}{1 - (\ell / \alpha'_{\ell n})^2} \frac{k}{\alpha'^2_{\ell n} \beta'_{\ell n}} \frac{F_{\ell}(\alpha'_{\ell n} a / b)}{J_{\ell}^2(\alpha'_{\ell n})}, \quad (19)$$

$$\beta'_{\ell n} = \sqrt{k^2 - (\alpha'_{\ell n} / b)^2}, \quad (20)$$

where $\alpha'_{\ell n}$ is the n th root of the derivative of J_{ℓ} , and where the orthogonality integral leading to Eq. (19) is given by Ref. 19. The asymptotic form of Eq. (19) for $n \gg 1$ is obtained using the relation²⁰

$$\alpha'_{\ell n} \simeq \pi(n - 3/4 + \ell/2), \quad n \gg 1, \quad (21)$$

which, in combination with Eq. (13), yields

$$A'_{\ell n} \simeq \frac{\rho_0 c_0 u_0}{1 - (\ell \Delta \zeta' / \pi \zeta')^2} \frac{\Delta \zeta'}{\zeta'} \frac{F_{\ell}(\zeta')}{\sqrt{1 - (\zeta' / ka)^2}}, \quad n \gg 1, \quad (22)$$

where $\zeta' = \pi(n - 3/4 + \ell/2)a/b$ and $\Delta \zeta' = \pi a/b$. In the limit $b \rightarrow \infty$, $\Delta \zeta'$ in Eq. (22) becomes $d\zeta'$, $\Delta \zeta'^2$ becomes $d\zeta'^2 = 0$, and the sum in Eq. (18) becomes an integral. Equation (16) [and hence Eq. (17)] is recovered by noting that ζ' is an integration variable and can be renamed ζ .

IV. RECOVERING THE RAYLEIGH INTEGRAL

To recover Eq. (2) from Eq. (17), express $J_{\ell}(k_r r)$ as²¹ $(2\pi)^{-1} \int_0^{2\pi} e^{i\ell\phi} e^{-ik_r r \sin\phi} d\phi$ and change variables to $\phi = \psi - \theta - \pi/2$:

$$p = \frac{k\rho_0 c_0}{2\pi} \int_0^{2\pi} \int_0^{\infty} u_0 F_{\ell}(k_r a) e^{i\ell(\psi - \pi/2)} e^{ik_r r \cos(\theta - \psi)} \frac{e^{ik_z z}}{k_z} \frac{dk_r}{k_r} d\psi. \quad (23)$$

Combining Eq. (1) with the integral representations of F_{ℓ} and J_{ℓ} shows that $u_0 F_{\ell}(k_r a) e^{i\ell(\psi - \pi/2)}$ equals $k_r^2 \mathcal{F}_{2D}\{u_z(r, \theta)\} / 2\pi$, where u_z is given by Eq. (1), reducing Eq. (23) to

$$p = \rho_0 c_0 k \mathcal{F}_{2D}^{-1}\{\mathcal{F}_{2D}[u_z(r, \theta)] e^{ik_z z} / k_z\}, \quad (24)$$

where \mathcal{F}_{2D} and \mathcal{F}_{2D}^{-1} are the polar forms of the spatial Fourier transform pair

$$\mathcal{F}_{2D}\{f\} = \hat{f} = \int_0^{2\pi} \int_0^{\infty} f(r, \theta) e^{-ik_r r \cos(\theta - \psi)} r dr d\theta, \quad (25)$$

$$\mathcal{F}_{2D}^{-1}\{\hat{f}\} = f = \frac{1}{4\pi^2} \int_0^{2\pi} \int_0^{\infty} \hat{f}(k_r, \psi) e^{ik_r r \cos(\theta - \psi)} k_r dk_r d\psi. \quad (26)$$

The Cartesian form of Eq. (24) describes propagation using Fourier acoustics,²² which by the convolution theorem can be expressed as

$$p = \rho_0 c_0 k \mathcal{F}_{2D}^{-1}\{\mathcal{F}_{2D}[u_z(x, y)]\} ** \mathcal{F}_{2D}^{-1}\{e^{ik_z z} / k_z\}, \quad (27)$$

where the double asterisk in Eq. (27) denotes convolution over x and y . Equation (27) is simplified by noting that $\mathcal{F}_{2D}^{-1}\{\mathcal{F}_{2D}[u_z(x, y)]\} = u_z(x, y)$ and $\mathcal{F}_{2D}\{e^{ik_r r} / r\} = i2\pi e^{ik_z |z|} / k_z$,²³ where $r = \sqrt{x^2 + y^2 + z^2}$:

$$p = -\frac{ik\rho_0 c_0}{2\pi} u_z(x, y) ** \frac{e^{ikr}}{r}. \quad (28)$$

By the definition of the convolution operation, Eq. (28) recovers Eq. (2) expressed in Cartesian coordinates, for which $\mathbf{r} = x\mathbf{e}_x + y\mathbf{e}_y + z\mathbf{e}_z$, $\mathbf{r}_0 = x_0\mathbf{e}_x + y_0\mathbf{e}_y$, and $dS_0 = dx_0 dy_0$, where \mathbf{e}_x , \mathbf{e}_y , and \mathbf{e}_z are the Cartesian unit vectors. The recovery of Eq. (2) from Eq. (3) shows that diffraction theory can be recovered from a modal solution in an infinitely large enclosure.

V. TWO EXAMPLES

The utility of Eq. (17) is demonstrated by two examples. In terms of the dimensionless parameters $P = p / \rho_0 c_0 u_0$, $R = r / a$, $Z = z / z_R$, and $K = ka$, where z_R is the Rayleigh distance $ka^2/2$, Eq. (16) becomes

$$P = e^{i\ell\theta} \int_0^{\infty} \frac{F_{\ell}(\zeta) J_{\ell}(\zeta R)}{\zeta \sqrt{1 - (\zeta/K)^2}} e^{iK^2 Z \sqrt{1 - (\zeta/K)^2} / 2} d\zeta. \quad (29)$$

Considered first is the axial pressure radiated by a planar circular piston obtained by setting $R = \ell = 0$, yielding¹³

$$\begin{aligned} P(Z) &= \int_0^{\infty} \frac{J_1(\zeta)}{\sqrt{1 - (\zeta/K)^2}} e^{iK^2 Z \sqrt{1 - (\zeta/K)^2} / 2} d\zeta \\ &= -iK I_{1/2}[-i\chi_-(Z)] K_{1/2}[-i\chi_+(Z)], \end{aligned} \quad (30)$$

where I_{ν} and K_{ν} are the ν th-order modified Bessel functions of the first and second kind, respectively, and where

$$\chi_{\pm}(Z) = (K/2) \left[\sqrt{1 + (KZ/2)^2} \pm KZ/2 \right]. \quad (31)$$

The relations^{13,14} $I_{\nu}(x) = i^{-\nu} J_{\nu}(ix)$, $K_{\nu}(ix) = \pi[I_{-\nu}(ix) - I_{\nu}(ix)] / (2 \sin \nu\pi)$, $J_{1/2}(x) = \sqrt{2x/\pi} \sin(x)/x$, and $J_{-1/2}(x) = \sqrt{2x/\pi} \cos(x)/x$ reduce Eq. (30) to

$$P(Z) = -2i \sin[\chi_-(Z)] e^{i\chi_+(Z)}, \quad (32)$$

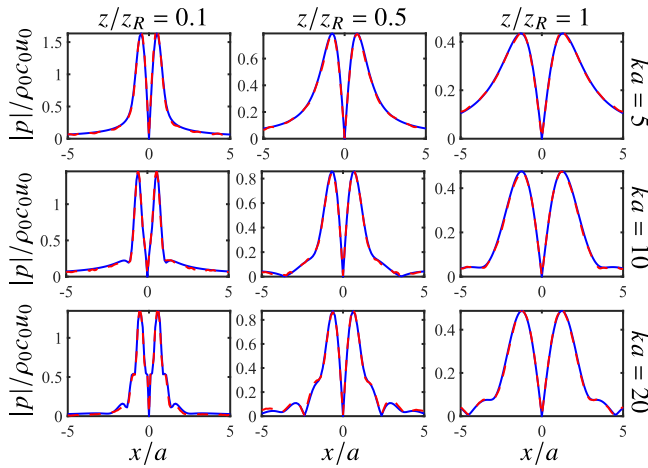


FIG. 2. Equation (17) (solid blue curves) compared with the Cartesian form of Eq. (24) (dashed red curves) for the source condition given by Eq. (1) with $\ell = 1$.

recovering the axial pressure radiated by a planar circular piston,⁸ which is traditionally derived by evaluating Eq. (2) for $|\mathbf{r} - \mathbf{r}_0| = \sqrt{r_0^2 + z^2}$ and $u_z = u_0 \text{circ}(r_0/a)$.

Considered next is the numerical evaluation of Eq. (29), which is compared with the angular spectrum method given by the Cartesian form of Eq. (24) used to create Fig. 2. The comparison is performed for $\ell = 1$, the orbital number most commonly used in vortex beam experiments.²⁴ The dashed red curves representing Eq. (24) were generated by carefully adjusting the domain and number of transverse discretization points to avoid errors due to aliasing.^{11,25–27} Numerical integration of Eq. (29), represented by the blue curves in Fig. 2, avoids the artifacts associated with simulation based on Fourier acoustics and is relatively easy to implement, making it advantageous over, but less general than, the evaluation of Eq. (24).

While analytical solutions of the paraxial equation are available in the far field $z \geq ka^2$ for sources described by Eq. (1),⁵ such solutions satisfactorily match the solution of the Helmholtz equation for $ka \geq 4\ell$, as discussed in Ref. 9. Studies involving near-field effects,^{28,29} high orbital numbers,³⁰ and/or vortex fields at low ka can therefore utilize the numerical evaluation of Eq. (29), which is an exact solution of the Helmholtz equation.

For sources described by Eq. (1), Eq. (29) can be obtained directly from Eq. (24) by replacing the Fourier transforms with ℓ th-order Hankel transforms. The advantages of Eq. (29) over Eq. (24) described above arise because the forward transform of Eq. (1) is evaluated analytically in Eq. (29) rather than numerically in Eq. (24).

VI. SUMMARY

The Rayleigh integral was derived for planar and vortex beam radiation from baffled circular pistons by considering a piston in an infinitely large cylindrical waveguide. While the traditional derivation of the Rayleigh integral requires knowledge of special functions, Green's functions, and the principle of

reciprocity,^{8,31} these concepts were not invoked in the present derivation. The simplicity came at the expense of the generality of the present derivation, which was restricted to circular piston sources. The Rayleigh integral was recast as a sum of Bessel beams, allowing for linear acoustic analyses involving individual Bessel beams to be generalized to radiation from sources described by Eq. (1). The formulation recovered the axial pressure due to a planar circular piston and was used to calculate the solution of the Helmholtz equation for a vortex beam with $\ell = 1$. Evaluation of the transformed diffraction integral in terms of the eigenfunctions of the Helmholtz equation was shown to avoid the artifacts associated with the numerical implementation based on Fourier acoustics.

ACKNOWLEDGMENTS

C.A.G. thanks Jackson S. Hallveld for showing him how to obtain Eq. (15) from Eq. (6), and for suggesting that Eq. (17) is equivalent to Eq. (24). C.A.G. was supported by the Applied Research Laboratories Chester M. McKinney Graduate Fellowship in Acoustics.

AUTHOR DECLARATIONS

Conflict of Interest

The authors have no conflicts to disclose.

DATA AVAILABILITY

The data that support the findings of this study are available from the corresponding author upon reasonable request.

¹L. Rayleigh, *The Theory of Sound* (MacMillan, London, UK, 1877), Vol. 2, Secs. 278 and 302.

²T. D. Mast and F. Yu, "Simplified expansions for radiation from a baffled circular piston," *J. Acoust. Soc. Am.* **118**, 3457–3464 (2005).

³S. Jiménez-Gambín, N. Jiménez, and F. Camarena, "Transcranial focusing of ultrasonic vortices by acoustic holograms," *Phys. Rev. App.* **14**, 054070 (2020).

⁴C. Ellouzi, A. Zabihi, F. Aghdasi, A. Kayes, M. Rivera, J. Zhong, A. Miri, and C. Shen, "Underwater double vortex generation using 3D printed acoustic lens and field multiplexing," *APL Mater.* **12**, 031130 (2024).

⁵C. A. Gokani, M. R. Haberman, and M. F. Hamilton, "Analytical solutions for acoustic vortex beam radiation from planar and spherically focused circular pistons," *JASA Express Lett.* **4**, 124001 (2024), Eqs. (7) and (8).

⁶B. T. Hefner and P. L. Marston, "An acoustical helicoidal wave transducer with applications for the alignment of ultrasonic and underwater systems," *J. Acoust. Soc. Am.* **106**, 3313–3316 (1999).

⁷V. Bollen and P. L. Marston, "Phase and amplitude evolution of backscattering by a sphere scanned through an acoustic vortex beam: Measured helicity projections," *J. Acoust. Soc. Am.* **148**, EL135–EL140 (2020), Eq. (1).

⁸A. D. Pierce, *Acoustics*, 3rd ed. (Springer, Cham, Switzerland, 2019), Eqs. (5.2.6) and (5.7.3).

⁹C. A. Gokani, M. R. Haberman, and M. F. Hamilton, "Paraxial and ray approximations of acoustic vortex beams," *J. Acoust. Soc. Am.* **155**, 2707–2723 (2024), Sec. IV and Appendix.

¹⁰P. L. Marston, "Scattering of a Bessel beam by a sphere: II. Helicoidal case and spherical shell example," *J. Acoust. Soc. Am.* **124**, 2905–2910 (2008), Eq. (1).

- ¹¹T. D. Daniel, F. Gittes, I. P. Kirsteins, and P. L. Marston, "Bessel beam expansion of linear focused ultrasound," *J. Acoust. Soc. Am.* **144**, 3076–3083 (2018), Eqs. (3) and (B5), Sec. IV, and Appendix C.
- ¹²D. T. Blackstock, *Fundamentals of Physical Acoustics* (Wiley, New York, 2000), Eqs. (11.A-14), (11A-36), and (12.B-10), Table 11.1, and p. 360.
- ¹³I. S. Gradshteyn and I. M. Ryzhik, *Table of Integrals, Series, and Products*, 4th ed. (Academic Press, New York, 1980), Items 6.637-1, 6.521-1, 8.406-3, 8.464-1, and 8.547.
- ¹⁴M. Abramowitz and I. A. Stegun, *Handbook of Mathematical Functions*, 4th ed. (Dover Publications, New York, 1972), Items 9.2.1, 9.6.2, and 11.1.1.
- ¹⁵J. Durkin, "Exact solutions for nondiffracting beams. I. The scalar theory," *J. Opt. Soc. Am. A* **4**, 651–654 (1987).
- ¹⁶P. L. Marston, "Scattering of a Bessel beam by a sphere," *J. Acoust. Soc. Am.* **121**, 753–758 (2007).
- ¹⁷L. V. King, "On the acoustic radiation field of the piezo-electric oscillator and the effect of viscosity on transmission," *Can. J. Res.* **11**, 135–155 (1934), Eq. (5).
- ¹⁸M. C. Junger and D. Feit, *Sound, Structures, and Their Interaction* (MIT Press, Cambridge, MA, 1986), Vol. 225, Eqs. (5.4) and (5.16).
- ¹⁹J. D. Jackson, *Classical Electrodynamics*, 1st ed. (Wiley, Hoboken, NJ, 1962), Prob. 3-8.
- ²⁰NIST Digital Library of Mathematical Functions, Item 10.21.20, <https://dlmf.nist.gov/10.21>.
- ²¹G. N. Watson, *A Treatise on the Theory of Bessel Functions*, 2nd ed. (Cambridge University Press, Cambridge, UK, 1944), Sec. 2.2, Eq. (5).
- ²²E. G. Williams, *Fourier Acoustics* (Academic Press, San Diego, CA, 1999), Sec. 2.9.
- ²³L. Brekhovskikh, *Waves in Layered Media*, 2nd ed. (Academic Press, Cambridge, MA, 1980), pp. 227–234.
- ²⁴S. Guo, Z. Ya, P. Wu, and M. Wan, "A review on acoustic vortices: Generation, characterization, applications and perspectives," *J. Appl. Phys.* **132**, 210701 (2022).
- ²⁵E. G. Williams and J. D. Maynard, "Numerical evaluation of the Rayleigh integral for planar radiators using the FFT," *J. Acoust. Soc. Am.* **72**, 2020–2030 (1982).
- ²⁶P. Wu, R. Kazys, and T. Stepinski, "Analysis of the numerically implemented angular spectrum approach based on the evaluation of two-dimensional acoustic fields. Part I. Errors due to the discrete Fourier transform and discretization," *J. Acoust. Soc. Am.* **99**, 1339–1348 (1996).
- ²⁷J. Blackmore, R. O. Cleveland, and J. Mobley, "Spatial filters suppress ripple artifacts in the computation of acoustic fields with the angular spectrum method," *J. Acoust. Soc. Am.* **144**, 2947–2951 (2018).
- ²⁸S. T. Kang and C.-K. Yeh, "Potential-well model in acoustic tweezers," *IEEE Trans. Ultrason. Ferroelectr. Freq. Control.* **57**, 1451–1459 (2010).
- ²⁹R. Lirette and J. Mobley, "Ultrasonic near-field based acoustic tweezers for the extraction and manipulation of hydrocarbon droplets," *Appl. Phys. Lett.* **121**, 244102 (2022).
- ³⁰M. E. Terzi, S. A. Tsysar, P. V. Yuldashev, M. M. Karzova, and O. A. Sapozhnikov, "Generation of a vortex ultrasonic beam with a phase plate with an angular dependence of the thickness," *Moscow Univ. Phys. Bull.* **72**, 61–67 (2017).
- ³¹P. M. Morse and K. U. Ingard, *Theoretical Acoustics* (McGraw-Hill, New York, 1968), Eqs. (7.1.17) and (7.4.6).